Copper nanoparticles synthesized in polymers by ion implantation: Surface morphology and optical properties of the nanocomposites

Vladimir N. Popok[a)]
Department of Physics and Nanotechnology, Aalborg University, Aalborg 9210, Denmark

Vladimir I. Nuzhdin and V.F. Valeev
Kazan Physical-Technical Institute, Russian Academy of Sciences, Kazan 420029, Russia

Andrei L. Stepanov
Kazan Physical-Technical Institute, Russian Academy of Sciences, Kazan 420029, Russia; Kazan Federal University, Kazan 420008, Russia; and Kazan National Research Technological University, Kazan 420015, Russia

(Received 6 June 2014; accepted 29 September 2014)

Polymethylmethacrylate (PMMA) and polyimide (PI) samples are implanted by 40 keV Cu^+ ions with high fluences to synthesize copper nanoparticles in shallow polymer layers. The produced metal/polymer nanocomposites are studied using atomic force and scanning electron microscopies as well as optical transmission spectroscopy. It is found that nucleation and growth of copper nanoparticles are strongly fluence-dependent as well as they are affected by the polymer properties, in particular, by radiation stability yielding different nanostructures for the implanted PI and PMMA. Shallow synthesized nanoparticles are observed to partly tower above the sample surface due to a side effect of high-fluence irradiation leading to considerable sputtering of polymers. Implantation and particle formation significantly change optical properties of both polymers reducing transmittance in the UV–visible range due to structural and compositional change as well as causing an absorption band related to localized surface plasmon resonance (LSPR) of the nanoparticles. The role of polymer type and its degradation under the implantation on LSPR is studied to optimize conditions for the formation of nanoplasmonic materials.

I. INTRODUCTION

In recent years, thin metal/polymer nanocomposite films attract considerable attention due to a number of practical applications.[1] In particular, by varying metal species and filling factor in a polymer one can control insulator-to-metal transition and provide evolution of mechanisms of electrical charge transport from variable range hopping toward electron conductance via percolating metal inclusions.[2–5] Applications combining electrical and mechanical properties of metal/polymer composites are of significant interest. Good examples are strain gages and elastomer electrodes.[6,7] Optical properties of polymers with gold, silver, and copper nanoparticles (NPs) are of significant interest due to localized surface plasmon resonance (LSPR).[8–11] These materials are considered to be promising for nanoscale plasmonics, fabrication of nonlinear optical devices, and optical sensors.[8,9,12]

Formation of metal/polymer composites can be performed by a variety of methods including particle formation by sputtering techniques, chemical and photo reduction, deposition from cluster beams or chemical solutions etc. One of the widely used methods is NP synthesis using ion implantation.[13] For the NP nucleation, the metal concentration must overcome the solubility limit in the polymer. Thus, high-fluence implantation is required. However, high fluences lead to radiation-induced transformation of the material due to the stopping of energetic ions and relatively low resistance of polymers with respect to irradiation.[14–16] There is scission of polymer chains and cross-linking under implantation. These phenomena are very much dependent on the irradiation conditions and type of polymer.[17] Breakage of chemical bonds causes degassing of volatile compounds, thus, leading to carbonization of the matrix. Extended systems with conjugated bonds are formed. Thus, metal ion implantation not only causes NP formation but also leads to dramatic change of the medium surrounding them. These phenomena have been extensively studied for the last two decades.[13,15–20]

From application-oriented point of view, one of the directions is ion synthesis of transition metal NPs in polymer substrates due to the interest in superparamagnetic and ferromagnetic properties that can be utilized for the development of magnetic data storage media and magnetosensors.[21–25] Another research area is related to the production of plasmonic materials by ion implantation of coinage metals in polymers. However, major complication for the ion synthesis of such materials is in

[a)]Address all correspondence to this author.
e-mail: vp@nano.aau.dk
DOI: 10.1557/jmr.2014.324

the polymer transformation from dielectric to conductor due to the formation of conjugated systems and high metal filling factor.[5,9,11,13] Such change in dielectric environment of NPs can lead to quenching of LSPR.[9] Therefore, accurate and delicate tuning of the implantation parameters as well as appropriate choice of polymer type are required to produce NPs and preserve LSPR.

In the current work, new data on the synthesis of copper NPs in polyimide (PI) and polymethylmethacrylate (PMMA) using very similar implantation conditions are presented. Structural and optical properties of both types of composites are compared and discussed. The research is focused on the optimization of implantation conditions for the formation of nanoplasmonic media with pronounced LSPR.

II. EXPERIMENTAL DETAILS

Commercial PI (Kapton) and PMMA with densities of 1.43 and 1.19 g cm^{-3}, respectively, were used for the ion synthesis. The samples were implanted by 40 keV Cu^+ ions with fluences $F = 1.0 \times 10^{16}$–1.2×10^{17} cm^{-2} at ion current densities j of 4 and 2.5 μA cm^{-2} for the former and latter polymers, respectively. The implantation was carried out in a residual vacuum of 10^{-5} Torr. To avoid thermal degradation, the sample holder was water-cooled and the temperature of the samples under the highest used implantation fluence did not exceed 370 K which is lower than the glass transition temperature T_g for both PI, which is between 633 and 683 K, and PMMA (T_g = 378 K).[26] PI does not have melting point while for PMMA it is 433 K, i.e., higher than T_g.[26,27]

Atomic force microscopy (AFM) study was carried out using Dimension 3000 (Digital Instruments Inc., Tonawanda, NY) and Ntegra Aura (NT-MDT, Zelenograd, Russia) devices. The measurements were performed in tapping mode using standard silicon cantilevers with curvature radius of tips ≤10 nm. For scanning electron microscopy (SEM) measurements JEOL JSM-6301F (JEOL Ltd., Tokyo, Japan) in secondary electron emission mode was utilized. To reduce charging of the samples, accelerating voltage below 5 kV was applied. Optical transmittance spectra were obtained using PerkinElmer High Performance Lambda 1050 spectrometer and standard procedure for the wave length interval between 250 and 800 nm.

III. RESULTS AND DISCUSSION

Ion implantation of PI results in both the disruption of phenyl rings and degradation of imide groups. The ether linkage degrades first and imide groups are gradually converted into amide ones with CO being the major gaseous emitted product.[17] Further evolution yields iminic- and pyridinic-like groups as well as tertiary amines,[18] thus, gradually converting the polymer exposed to high-fluence implantation toward the structure with extended polycondensed systems as proposed in Ref. 28 and shown in Fig. 1. The chemical structure of PMMA is presented in Fig. 2. Ion implantation of this polymer is known to cause scission of chains, for instance, at the oxygen-containing group and between the carbon in the backbone and in CH_2 group yielding low molecular weight species that can easily evaporate.[29] Thus, free radical formation and degassing promote cross-linking and depolymerization transforming PMMA into a structure with heavily carbonized areas consisting of aromatic rings (as shown in Fig. 2) having minor inclusions of residual PMMA. In other words, the implanted PMMA layer evolves into pyrolytic carbon-like structure. By comparing the degradation schemes for PI and PMMA, it can be concluded that structure and composition of both polymers significantly evolve under the ion implantation. However, PI is known to have higher resistance against radiation compared to PMMA.[15,30]

AFM images of the PI and PMMA surfaces are shown in Figs. 3 and 4, respectively. Typical roughness of unimplanted samples is found to be around 2 nm for both polymers and 2 × 2 μm areas. Sometimes it is possible to see trenches or ridges as shown, for example, for PMMA in Fig. 4(a). These features can locally increase the roughness. For this scanned area, the root mean square value (RMS) is found to be 2.7 nm. Implantation with $F = (1.0–2.5) \times 10^{16}$ cm^{-2} does not lead to significant changes in the PI surface morphology compared to the

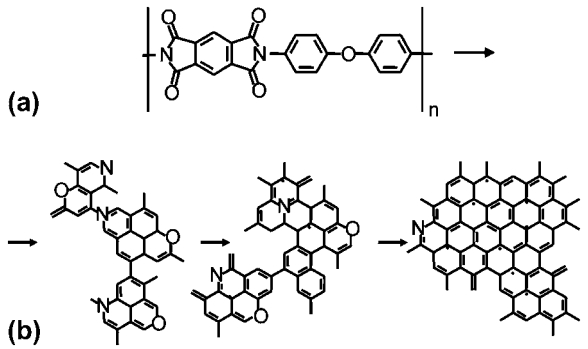

FIG. 1. (a) Chemical structure of pristine PI and (b) final evolution of PI under high-fluence ion implantation. For more details about intermediate transformation stages see the text.

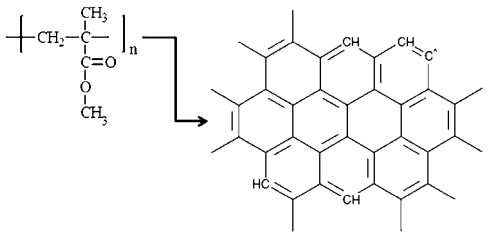

FIG. 2. Chemical structure of PMMA and final evolution of PMMA under high-fluence ion implantation. For more details about intermediate transformation stages see the text.

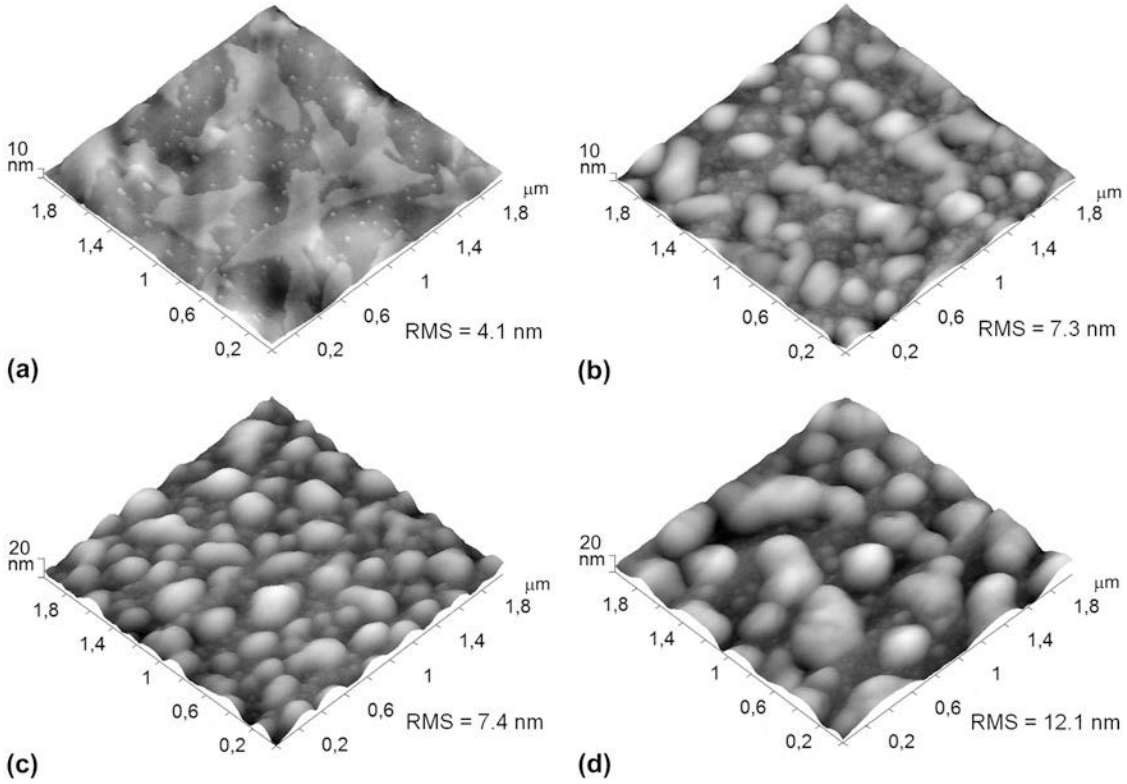

FIG. 3. 3D AFM images of PI implanted by Cu^+ ions with fluences of (a) 2.5×10^{16} cm^{-2}, (b) 5.0×10^{16} cm^{-2}, (c) 7.5×10^{16} cm^{-2}, and (d) 1.0×10^{17} cm^{-2}. RMS represents root mean square values for surface roughness.

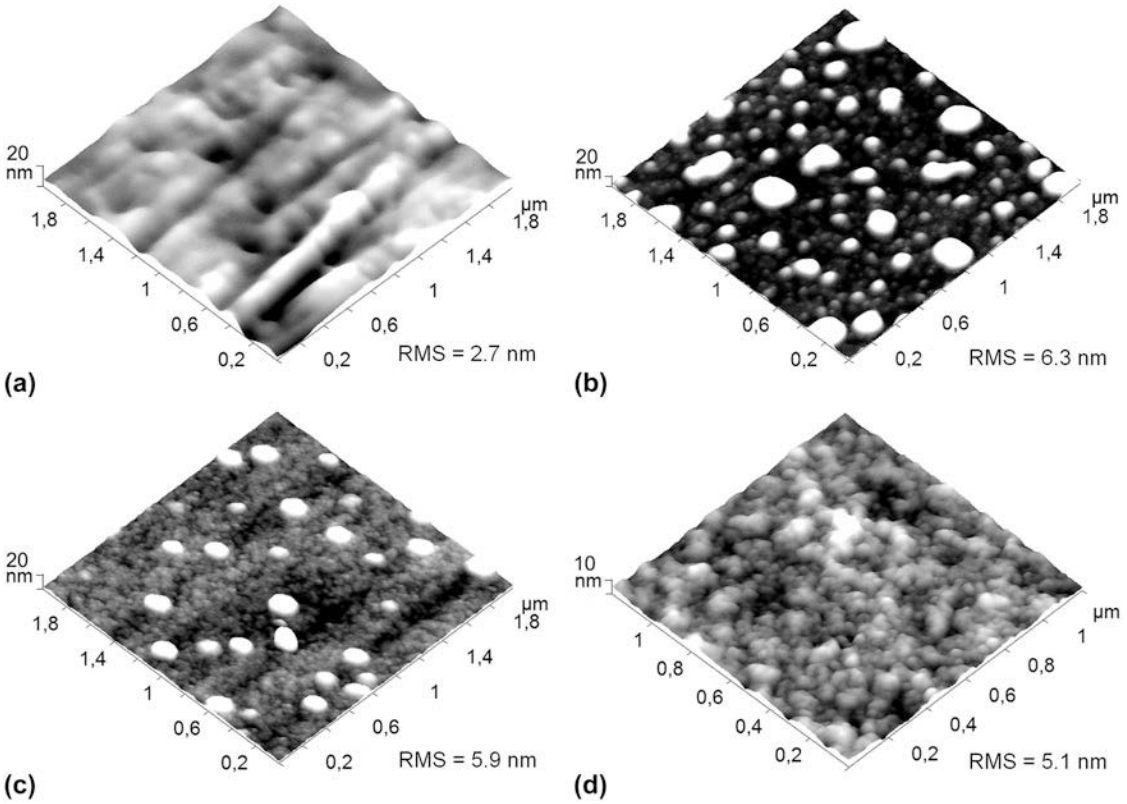

FIG. 4. 3D AFM images of (a) pristine PMMA and PMMA implanted by Cu^+ ions with fluences of (b) 5.0×10^{16} cm^{-2}, (c) 1.0×10^{17} cm^{-2}, and (d) 1.2×10^{17} cm^{-2}. RMS represents root mean square values for surface roughness.

pristine polymer except appearance of a few nanometer high bumps as can be seen in Fig. 3(a). Fluence increase up to (5.0–7.5) $\times$ 10^{16} cm^{-2} causes significant restructuring of the PI surfaces. They become much rougher (see RMS values in the panels) and formation of numerous small bumps that cover entire implanted surface is observed. Along with small bumps larger features with a height of 20–40 nm and lateral basal dimensions of 100–300 nm are observed on the PI surfaces [see Figs. 3(b) and 3(c)]. Modification of the surface morphology is qualitatively very similar for PMMA as one can see by comparing panel (b) of Fig. 3 with panel (b) of Fig. 4 corresponding to the same fluence. For PI implanted to higher fluences there is no qualitative change in the surface topography as can be seen by comparison of Figs. 3(c) and 3(d) except that the roughness is increased. However, for PMMA, number of large bumps is decreased with fluence and they are not observed for $F = 1.2 \times 10^{17}$ cm^{-2} [compare Figs. 4(b)–4(d)]. This tendency leads to appropriate decrease of RMS.

It is well known that low-energy implantation to fluences above approximately 1.0×10^{16} cm^{-2} leads to nucleation of metal NPs in thin polymer layer.[10,13] Earlier studies showed that thickness of the modified layer slightly varies depending on the polymer type and metal ion species, but for energies of 30–40 keV typically does not exceed a few tens of nanometers with the maximum metal concentration located at very low depth.[13,31,32] Assuming that NP growth occurs by successive joining of single metal atoms one can conclude that the nucleation process is governed by the local copper concentration. Therefore, NPs are formed at the depth corresponding to the highest copper concentration, i.e., in the very shallow layer. However, high-fluence ion implantation leads not only to the NP nucleation but also causes sputtering of the polymer surface.[13] Sputtering rates of polymer materials used in these experiments are few times higher compared to copper atoms incorporated into substrate during the implantation. Since metal NPs are very shallowly located, sputtering of thin polymer layer at later stage of implantation may originate the towering of

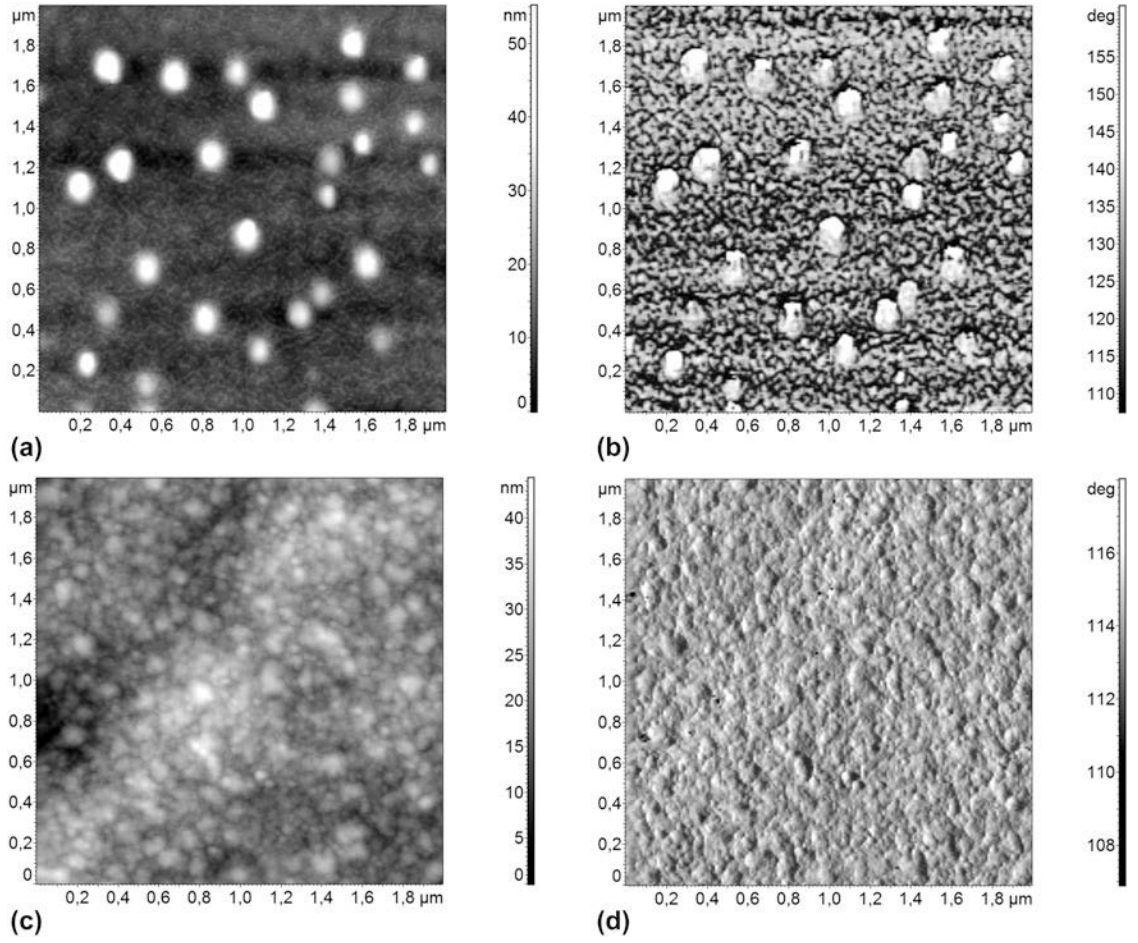

FIG. 5. 2D AFM images of PMMA implanted by Cu^{+} ions. Panels (a) and (b) correspond to fluence of 1.0×10^{17} cm^{-2} showing height (topography) and phase scans, respectively. Panels (c) and (d) correspond to fluence of 1.2×10^{17} cm^{-2} showing height (topography) and phase scans, respectively.

already formed (at earlier stage of implantation) NPs. This scenario was proved for a number of materials like SiO_2, sapphire, etc. implanted by different metal ions. See for example Ref. 33. Thus, a number of tiny bumps with a height of few nanometers visible in Fig. 3(a) can be a consequence of such sputtering and appearance of some NPs on the surface.

Increase of implantation fluence leads to the increase of particle density, and many NPs become partly towered above the surface as can be seen in Figs. 3(b) and 4(b). Along with small bumps representing individual NPs, the larger features are observed for both polymers. They are shown in Figs. 3(b) and 3(c), Figs. 4(b) and 4(c) and can be assigned to agglomeration or coagulation of copper NPs. The association of the bumps with NPs is confirmed by the agreement between the topography and phase AFM images. They are presented for selected fluences and PMMA in Fig. 5 to be able to make direct comparison for the exactly same area. One can clearly see that the bumps associated with NPs in topography are well reproduced by the phase change. Further support is obtained using SEM study where clear contrast between the metal-rich (bright) areas and the rest of the surface is observed (see Fig. 6 as an example). Size of bright regions in SEM images is found to be in good agreement with lateral dimensions of the bumps observed by AFM for the corresponding implantation fluence [compare Figs. 3(b) and 6]. Unfortunately, AFM does not allow detailed statistical study of NP sizes because it is not known for how much a particle is towered above the surface. It can be ¼, 1/3, ½, or other fraction of the diameter.

One can see that the morphology of the sample surfaces is very similar for both types of polymers at moderate fluences ($\sim 10^{16}$ cm^{-2}), i.e., one can suggest quite similar mechanisms for NP formation in PI and PMMA. However, at very high fluences, large bumps associated with coagulates of NPs start disappearing in PMMA and they are not observed for the highest fluence of 1.2×10^{17} cm^{-2}. Such change can be explained through the consideration of properties of the pristine polymers. PMMA has much lower T_g compared to PI. High fluences mean longer implantation time compared to moderate ones, i.e., rise of mean temperature of the polymer surface can be assumed. As mentioned in the section "Experimental details", the mean sample temperature under the very high-fluence regimes reaches the values very close to T_g of PMMA while it is much below of T_g for PI. Thus, heating of the PMMA samples can lead to softening of the material and change its viscosity. It was shown elsewhere that metal implantation into polymers with high viscosity affects the diffusion mobility of metal atoms, thus, leading to more homogeneous distribution that hampers coagulation into large granules.[34] This may very well be the reason in our case. Softening of PMMA under very high fluences prevents Ostwald ripening and formation of large agglomerates of NPs while for PI the softening is lower and the agglomerates can form.

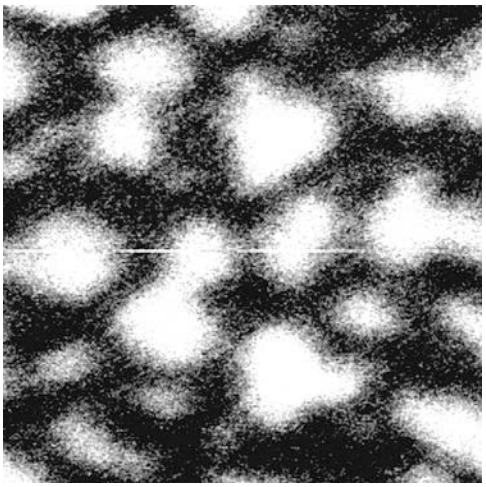

FIG. 6. SEM image of PI implanted by Cu^+ ions with fluence of 5.0×10^{16} cm^{-2}. Image size is 2×2 μm.

Visually, both polymers change to brown color under the implantation and acquire metallic luster at the highest fluences. The change in color is related to the carbonization accompanied by the formation of conjugated bonds due to the above-described structural evolution. Optical transmission spectra of the Cu-implanted PI and PMMA samples are presented in Figs. 7 and 8, respectively. Ion implantation drastically decreases transmittance of the samples in the UV–visible interval of spectrum that is related to the evolution of polymer structure and composition, in particular causing a decrease of optical gap. This is a well-known phenomenon extensively studied for different polymers and various ion species (see for example Refs. 15,17,18,25 and references therein), and therefore, we do not address it further.

Our focus is on the study of plasmonic properties of NPs. In Figs. 7 and 8, an absorption band with minimum of transmittance between approximately 610 and 640 nm for both implanted PI and PMMA is seen. The band becomes pronounced for PI at $F \geq 5.0 \times 10^{16}$ cm^{-2}. For PMMA, it is present only for the highest fluence. The band can be assigned to LSPR on copper NPs.[35,36] However, this LSPR band is relatively weak and broad that is related to the NP environment in the radiation-damaged polymers, i.e., to the dramatic change of dielectric function under the implantation due to the conversion of shallow polymer layers into amorphous carbon-like material. The irradiation causes significant carbonization that leads to dumping of the LSPR extinction and causes the band broadening.[9,31]

From AFM study, it was suggested that NP formation under the implantation with moderate fluences was very

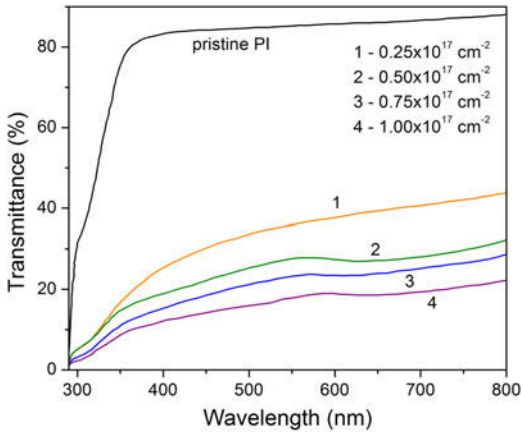

FIG. 7. Optical transmission spectra of pristine and ion-implanted PI. Fluences are shown in the panel.

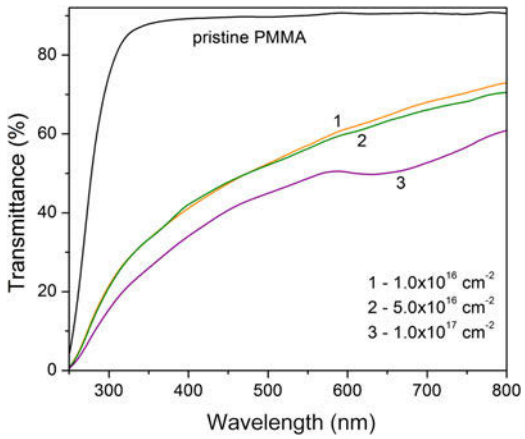

FIG. 8. Optical transmission spectra of pristine and ion-implanted PMMA. Fluences are shown in the panel.

similar in both polymers. Hence, one can expect similar optical properties related to the copper NPs. However, by comparing the spectra presented in Figs. 7 and 8, one can see that LSPR band is observed in PI for lower fluences, starting from 5.0×10^{16} cm^{-2}, compared to PMMA where the band is found for the highest fluence only. Reason for the quenching of LSPR in PMMA for moderate fluences is not very clear. It can be related to the difference in electronic properties of the radiation-modified PI and PMMA. For example, the formation of high-conductive medium (due to more efficient conjugation) surrounding the particles in PMMA and, thus, leading to the dumping of the resonance can be suggested as a possible reason. However, this phenomenon requires further detailed investigation. On the other hand, the band observed for the implanted PMMA is sharper compared to the PI cases. This fact is most probably related to PMMA softening causing more homogeneous metal distribution and lower size dispersion of NPs as suggested while discussing the AFM results.

IV. CONCLUSIONS

The PI and PMMA samples with ion-synthesized Cu NPs were studied using a few experimental techniques. It was found that particles have been formed in the shallow polymer layers and sputtering of the polymer target as a side effect of high-fluence implantation caused partial towering of NPs located just beneath the surface. NP nucleation and growth were strongly affected by the implantation parameters and polymer evolution under the implantation. It was suggested that relatively low radiation stability of PMMA can cause its softening upon implantation leading to more homogeneous metal distribution, thus, preventing Ostwald ripening and formation of particle agglomerates or coagulates. More homogeneous metal distribution and lower size dispersion of NPs lead to relatively sharp LSPR band in the case of PMMA implanted with fluence of 1.2×10^{17} cm^{-2}. Thus, by considering the structure and composition of pristine polymer as well as its degradation under the implantation one can find appropriate materials for the synthesis of metal/polymer nanocomposites with required parameters for optical applications.

ACKNOWLEDGMENTS

This work was partly supported by the Russian Foundation for Basic Research (Nos. 12-02-97029 and 12-02-00528). A.L. Stepanov acknowledges the financial support of the Russian Scientific Foundation (No. 14-13-00758).

REFERENCES

1. K.I. Winey and R.A. Vaia: Polymer nanocomposites. *MRS Bull.* **32**, 314–319 (2007).
2. P.A. Lee and T.V. Ramakrishan: Disordered electronic systems. *Rev. Mod. Phys.* **57**, 287–337 (1985).
3. G. Du, A. Burns, V.N. Prigodin, C.S. Wang, J. Joo, and A.J. Epstein: Anomalous Anderson transition in carbonized ion-implanted polymer p-phenylenebenzobisoxazole. *Phys. Rev. B* **61**, 10142–10148 (2000).
4. Y. Wang, L.B. Bridwell, and R.E. Giedd: Composite conduction in ion-implanted polymers. *J. Appl. Phys.* **73**, 474–476 (1993).
5. F.S. Teixeira, M.C. Salvadori, M. Cattani, and I.G. Brown: Gold-implanted shallow conducting layers in polymethylmethacrylate. *J. Appl. Phys.* **105**, 064313 (2009).
6. G. Di Girolamo, M. Massaro, E. Piscopiello, and L. Tapfer: Metal ion implantation in inert polymers for strain gauge applications. *Nucl. Instrum. Methods. Phys. Res., Sect. B* **268**, 2878–2882 (2010).
7. G. Corbelli, C. Ghisleri, M. Marelli, P. Milani, and L. Ravagnan: Highly deformable nanostructured elastomeric electrodes with improving conductivity upon cyclical stretching. *Adv. Mater.* **23**, 4504–4508 (2011).
8. Ch. Buhal, S.P. Withrow, C.W. White, and D.B. Poker: Ion implantation of optical materials. *Annu. Rev. Mater. Sci.* **24**, 125–157 (1994).
9. A.L. Stepanov: Optical extinction of metal nanoparticles synthesized in polymer by ion implantation. In *Metal-polymer Nanocomposites*, L. Nicolais and G. Garotenuto eds.; John Wiley & Sons: Hoboken, 2005; pp. 241–263.

10. A.L. Stepanov: Synthesis of silver nanoparticles in dielectric matrix by ion implantation: A review. *Rev. Adv. Mater. Sci.* **26**, 1–29 (2010).
11. A.L. Stepanov, V.N. Popok, I.B. Khaibullin, and U. Kreibig: Optical properties of polymethylmethacrilate with implanted silver nanoparticles. *Nucl. Instrum. Methods Phys. Res., Sect. B* **191**, 473–477 (2002).
12. S.A. Maier, P.G. Kik, L.A. Sweatlock, and H.A. Atwater: Energy transport in metal nanoparticle plasmon waveguides. *Mater. Res. Soc. Symp. Proc.* **777**, (2003) T7.1.1–7.1.12.
13. V.N. Popok: Ion implantation of polymers: Formation of nanoparticulate materials. *Rev. Adv. Mater. Sci.* **30**, 1–26 (2012).
14. T. Venkatesan, L. Calcagno, B.S. Elman, and G. Foti: Ion beam effects in organic molecular solids and polymers. In *Ion Beam Modification of Insulators*, P. Mazzoldi and G.W. Arnold eds.; Elsevier: Amsterdam, 1987; pp. 301–379.
15. V.N. Popok: Compositional and Structural Alterations of Polymers under Low-to-medium-energy Ion Implantation. In *Surface Science Research*, Ch.P. Norris ed.; Nova Sci. Publ.: New York, 2005; pp. 147–193.
16. M. Behar and D. Fink: Mechanisms of particle-polymer interaction. In *Fundamentals of Ion-irradiated Polymer*, D. Fink ed.; Springer: Berlin, 2004; pp. 119–169.
17. D.V. Sviridov: Chemical aspects of implantation of high-energy ions into polymeric materials. *Russ. Chem. Rev.* **71**, 315–327 (2002).
18. D.V. Sviridov, V.B. Odzhaev, and I.P. Kozlov: Ion-implanted polymers. In *Electrical and Optical Polymer Systems*, D.L. Wise, G.E. Wnek, D.J. Trantolo, Th.M. Cooper, and J.D. Gresser eds.; Marcel Dekker: New York, 1998; pp. 387–422.
19. G. Marletta and F. Iacona: Chemical and physical property modifications induced by ion irradiation of polymers. In *Materials and Processes for Surface and Interface Engineering*, Y. Pauleau ed.; Kluwer: Dordrecht, 1995; pp. 597–640.
20. A. Kondyurin and M. Bilek: *Ion Beam Treatment of Polymers* (Elsevier, Amsterdam, 2008).
21. V.Yu. Petukhov, N.R. Khabibullina, M.I. Ibragimova, A.A. Bukharaev, D.A. Biziaev, E.P. Zheglov, G.G. Gumarov, and R. Muller: Magnetic properties of thin metal-polymer films prepared by high-dose ion-beam implantation of iron and cobalt ions into polyethylene terephthalate. *Appl. Magn. Reson.* **32**, 345–361 (2007).
22. R.I. Khaibullin, V.N. Popok, V.V. Bazarov, E.P. Zheglov, B.Z. Rameev, C. Okay, L.R. Tagirov, and B. Aktas: Ion synthesis of iron granular films in polyimide. *Nucl. Instrum. Methods Phys. Res., Sect. B* **191**, 810–814 (2002).
23. R.I. Khaibullin, B.Z. Rameev, C. Okay, A.L. Stepanov, V.A. Zhikharev, I.B. Khaibullin, L.R. Tagirov, and B. Aktas: Ion beam synthesis of magnetic nanoparticles in polymers. In *Nanostructured Magnetic Materials and their Applications, NATO Science Series: II Mathematics, Physics and Chemistry*, B. Aktas, L. Tagirov, and F. Mikailov eds.; Kluwer: Dordrecht, Vol. **143**, 2004; pp. 33–64.
24. A. Mackova, P. Malinsky, R. Miksova, H. Pupikova, R.I. Khaibullin, V.F. Valeev, V. Svorcik, and P. Slepicka: Annealing of PEEK, PET and PI implanted with Co ions to high fluences. *Nucl. Instrum. Methods Phys. Res., Sect. B* **307**, 598–602 (2013).
25. A. Mackova, P. Malinsky, R. Miksova, V. Hnatowicz, R.I. Khaibullin, P. Slepicka, and V. Svorcik: Characterisation of PEEK, PET and PI implanted with 80 keV Fe ions to high fluences. *Nucl. Instrum. Methods Phys. Res., Sect. B* **331**, 176–181 (2014).
26. *Handbook of Chemistry and Physics*, W.M. Haynes ed., CRC Press: Boca Raton, 2013.
27. M. Ding: Isomeric polyimides. *Prog. Polym. Sci.* **32**, 623–668 (2007).
28. V.N. Popok, I.I. Azarko, R.I. Khaibullin, A.L. Stepanov, V. Hnatowicz, A. Mackova, and S.V. Prasalovich: Radiation-induced change of polyimide properties under high-fluence and high ion current density implantation. *Appl. Phys. A* **78**, 1067–1072 (2004).
29. A. Kondyurin and M. Bilek: Etching and structure changes in PMMA coating under argon plasma immersion ion implantation. *Nucl. Instrum. Methods Phys. Res., Sect. B* **269**, 1361–1369 (2011).
30. V.N. Popok, I.I. Azarko, V.B. Odzhaev, A. Toth, and R.I. Khaibullin: High fluence ion beam modification of polymer surfaces: EPR and XPS study. *Nucl. Instrum. Methods Phys. Res., Sect. B* **178**, 305–310 (2001).
31. A.L. Stepanov, S.N. Abdullin, V.Yu. Petukhov, Yu.N. Osin, R.I. Khaibullin, and I.B. Khaibullin: Formation of metal-polymer composites by ion implantation. *Philos. Mag. B* **80**, 23–28 (2000).
32. W. Yuguang, Z. Tonghe, Z. Yawen, Z. Gu, Z. Huixing, and Z. Xiaoji: Influence of nanostructure on electrical and mechanical properties for Cu implanted PET. *Surf. Coat. Technol.* **148**, 221–225 (2001).
33. V.N. Popok, A.V. Gromov, V.I. Nuzhdin, and A.L. Stepanov: Optical and AFM study of ion-synthesised silver nanoparticles in thin surface layers of SiO_2 glass. *J. Non-Cryst. Solids* **356**, 1258–1261 (2010).
34. S.N. Abdullin, A.L. Stepanov, Y.N. Osin, R.I. Khaibullin, and I.B. Khibullin: Synthesis of metallic dispersion and continuous films in the viscous polymer by implantation of cobalt ions. *Surf. Coat. Technol.* **106**, 214–219 (2001).
35. R.F. Ganeev, A.I. Ryasnyansky, A.L. Stepanov, and T. Usmanov: Saturated absorption and reverse saturated absorption of Cu:SiO_2 at λ=532 nm. *Phys. Status Solidi B* **241**, R1–R4 (2004).
36. A.L. Stepanov, V.N. Popok, D.E. Hole, and I.B. Khaibullin: Ion synthesis and laser annealing of Cu nanoparticles in Al_2O_3. *Appl. Phys. A* **74**, 441–446 (2002).